Diastereoselectivity in the Reaction of $RCH_2C[CH_2P(Ar)(Li)]_3$ with Electrophiles: Enhancement of Diastereoselective Control by η^3-Coordination in $\{RCH_2C[CH_2P(Ar)(Li)]_3\}Mo(CO)_3$

Michael Büchner, Gottfried Huttner*, Ute Winterhalter, and Axel Frick

Anorganisch-Chemisches Institut, Universität Heidelberg,
Im Neuenheimer Feld 270, D-69120 Heidelberg, Germany

Received June 6, 1997

Keywords: Chiral tripod ligands / Tripod $Mo(CO)_3$ compounds / Diastereoselective synthesis / Separation of diastereomers

Following a procedure developed for $H_3CC[CH_2P(Ph)_2]_3$ (**1a**) as the starting compound, various tripod ligands $RCH_2C[CH_2P(Ar)_2]_3$ (**1**) have been transformed into the trilithiotriphosphides $RCH_2C[CH_2P(Ar)(Li)]_3$ by reductive cleavage of their P–Ar bonds by metallic lithium. The triphosphides are readily protonated to produce $RCH_2C[CH_2P(Ar)(H)]_3$ (**2**). Reaction of $RCH_2C[CH_2P(Ar)(Li)]_3$ with various electrophiles R′–Hal leads to the two diastereomers of $RCH_2C[CH_2P(Ar)(R')]_3$ (**6**) with an (*RRR/SSS* : *RRS/SSR*) ratio close to the statistical value of 1:3, except when Ar = Ph and R′ = Bzl, where the *RRS/SSR* diastereomer is obtained almost exclusively. In contrast, the reaction of $\{RCH_2C[CH_2P(Ar)(Li)]_3\}Mo(CO)_3$ (**4**) with electrophiles R′–Hal tends to favour the formation of the homochiral *RRR/SSS* diastereomers. The triphosphide coordination compounds **4** are available by two different routes: either the complexes $\{RCH_2C[CH_2P(Ar)(H)]_3\}Mo(CO)_3$, obtained from **2** and $(CH_3CN)_3Mo(CO)_3$, are deprotonated by MeLi, or the trilithiotriphosphides $RCH_2C[CH_2P(Ar)(Li)]_3$ are reacted with $(CH_3CN)_3Mo(CO)_3$ to produce **4** in high yields. The ratio in which the two diastereomeric forms of **5** are obtained depends on the nature of the electrophile: the greatest diastereomeric discrimination is obtained for Ar = Ph, R = Ph, R′ = Bzl, where the homochiral *RRR/SSS* enantiomeric pair is produced in a fourfold excess relative to the *RRS/SSR* pair. Two-dimensional NMR spectra and simulations of one-dimensional spectra are used to ascertain the diastereomeric excess in each case. X-ray analyses of three compounds of type **5** (**5d**, Ar = Ph, R = H, R′ = Bzl; **5k**, Ar = 3,5-$Me_2C_6H_3$, R = H, R′ = Bzl; **5l**, Ar = Ph, R = Ph, R′ = Bzl) indicate the remarkable conformational stability of the tripod metal scaffolding, with the conformations observed for these three compounds in three different solid-state environments being closely similar, even with respect to the torsional arrangement of the phosphorus-bound benzyl groups.

Introduction

Tripod ligands [$RCH_2C(CH_2X)(CH_2Y)(CH_2Z)$, X, Y, Z = donor functions e.g. PR'_2], form tripod metal templates tripod-M with transition metals M. In these templates, the chelate cage formed by the tripod ligand completely shields the metal on one side. At the same time, the remaining coordination space on the other side will be cast into a specific and predictable shape by the substituents R′ at the donor atoms[1]. These substituents form a kind of pocket, which shields the coligands L in compounds of the type tripod-ML_n. The fact that this shielding can be exploited in a productive way in coordination chemistry has been extensively documented by Sacconi and co-workers[2]. It has also been demonstrated that in spite of, or possibly because of this shielding, tripod metal templates show a specific catalytic reactivity[3]. Bringing together these two properties – the potential to shape the coordination half-space in tripod-M templates and the catalytic activity of these templates – should allow for an analysis of the correlation between catalytic activity and the shape of ligand-metal entities for this class of compounds. In order to explore such correlations it is necessary to develop syntheses that allow for a convergent preparation of tripod ligands [$RCH_2C(CH_2X)(CH_2Y)(CH_2Z)$, X, Y, Z = donor functions] with a broad variety of donor groups. Such syntheses have been developed[4] and even enantioselective syntheses of C_1 symmetric chiral tripod ligands of the type $RCH_2C(CH_2PR'_2)(CH_2PR''_2)(CH_2PR'''_2)$ have been described[5].

Another means of introducing chirality into tripod ligands involves embedding the chirality into the donor functions themselves. This approach has been used in a few examples relying on the selective introduction of chiral PRR′-groups into the tripod scaffolding[6][7].

An alternative route to tripod ligands containing chiral phosphane donor groups is based on the selective cleavage of phosphorus-aryl bonds in RR′P-aryl compounds, thus relying on the seminal work of Issleib and co-workers[8]. This strategy has been used by other groups for the synthesis of (H)(Ph)PCH_2CH_2P(Ph)(H) and related compounds[9]. Based on the work of the Issleib group, it has been shown that the tripod ligand $H_3CC[CH_2P(Ph)_2]_3$ is selectively transformed into $H_3CC[CH_2P(Ph)(Li)]_3$, which upon the reaction with organic electrophiles R–Hal produces tripod ligands $H_3CC[CH_2P(Ph)(R)]_3$[10][11]. It has been found that, in general, both diastereomeric forms, the enantiomeric pair *RRR/SSS* and the pair *RRS/SSR*, are obtained in a statistical ratio of 1:3. Only in the case of

 © WILEY-VCH Verlag GmbH, D-69451 Weinheim, 1997 0009-2940/97/1010-1379 $ 17.50+.50/0

BzlCl as the electrophile was diastereomeric discrimination observed, leading to an almost exclusive formation of the *RRS/SSR* diastereomer[11]. This diastereomeric discrimination was attributed to the cage structure of $H_3CC[CH_2P(Ph)(Li)]_3$, which allows for an efficient transcription of chiral information[11]. With this argument in mind, a logical extension would be to assume that this type of information pathway would even be more efficient if the three phosphido groups of $CH_3C[CH_2P(Ph)(Li)]_3$ could be linked to a transition metal before treating them with an electrophile. Since the chemistry of $\{H_3CC[CH_2P(Ph)(R)]_3\}Mo(CO)_3$ has already been investigated[11], the $Mo(CO)_3$ fragment appeared to be the linker of choice. It is shown herein that $\{RCH_2C[CH_2P(Ar)(Li)]_3\}Mo(CO)_3$ (**4**) is in fact an easy to obtain type of compound. The trilithio species **4** are easily protonated to yield $\{RCH_2C[CH_2P(Ar)(H)]_3\}Mo(CO)_3$ (**3**). The diastereomers *RRR/SSS*-**3** and *RRS/SSR*-**3** are formed in the statistical ratio of 1:3. In contrast, the reaction of **4** with organic electrophiles R−Hal reveals a significant diastereoselective control. With BzlCl as the electrophile, the *RRR/SSS*-diastereomer, disfavoured on statistical grounds, is actually formed in large excess.

Results and Discussion

The tripod ligands $RCH_2C[CH_2P(Ar)_2]_3$ are easily available by published procedures[12]. Following the general approach of Issleib[8], it has been shown that **1a** may be transformed into its trilithio derivative which, upon hydrolysis, affords the tripod ligand **2a**[11]. The same pattern of reactivity is observed for all the other compounds **1**, irrespective of the specific kind of aryl group (Figure 1).

Figure 1. Preparation of compounds **2**

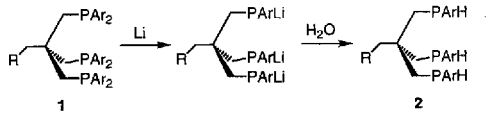

Nr.	R	Ar
1a, 2a	H	Ph
1b, 2b	H	4-MeC_6H_4
1c, 2c	H	2-MeC_6H_4
1d, 2d	H	3,5-$Me_2C_6H_3$
1e, 2e	Ph	Ph

The colourless THF solutions of compounds **1** are transformed into dark-red solutions, containing the trilithiotriphosphides (Figure 1), upon reaction with an excess of lithium metal. The reactions are complete after stirring for 20 hours at 20°C. The triphosphides[11] are not isolated as such, but are transformed into the monoarylphosphanylmethyl derivatives **2**. Compounds **2** are isolated as colourless oils from the THF extracts after evaporation of the solvent. They are of sufficient purity for further reactions. Compound **2a** has been described previously[11]. Correct elemental analyses are obtained for **2d** and **2e**, while **2b** and **2c** tenaciously retain THF. Attempts at further purification by chromatography or by applying elevated temperatures for the removal of THF have not been successful owing to partial decomposition of the compounds under these conditions. All of the compounds **2** give clear-cut mass spectra (Table 1) as well as NMR spectra (Tables 2 and 3), which are fully consistent with the assigned structures. Mass spectra under EI conditions show prominent signals for $[M^+ - H]$ in each case and the expected fragmentation patterns (Table 1).

Table 1. MS (EI) data of compounds **2**

No.	(*m/z*) (%)	(*m/z*) (%)	(*m/z*) (%)
2b	437 (50)	347 (55)	315 (100)
	$[M^+ - H]$	$[M^+ - C_7H_7]$	$[M^+ - P(C_7H_7)(H)]$
2c	437 (20)	347 (100)	315 (45)
	$[M^+ - H]$	$[M^+ - C_7H_7]$	$[M^+ - P(C_7H_7)(H)]$
2d	479 (100)	375 (52)	343 (62)
	$[M^+ - H]$	$[M^+ - C_8H_9]$	$[M^+ - P(C_8H_9)(H)]$
2e	471 (30)	395 (66)	363 (100)
	$[M^+ - H]$	$[M^+ - Ph]$	$[M^+ - P(Ph)(H)]$

The ^{1}H-NMR spectra of the ligands **2** are not completely resolved at 200 MHz (Table 2). The aryl residues and the substituents lead to clearly defined signals (Table 2). However, due to their multiple diastereotopic differentiation (chirality at the neighbouring phosphorus and chirality induced by the two other phosphorus centers), the methylene protons give rise to overlapping multiplets, even with phosphorus decoupling; the presence of six such protons is clearly evident (Table 2), but individual assignments are not possible. The signals for the methyl groups of **2b−d**, as well as the benzyl CH_2 group (**2e**), are clearly separated and can be assigned (Table 2). The phosphorus-bound protons appear as doublets (**2b−d**), with a $^1J_{HP}$ coupling of around 210 Hz (Table 2). Each doublet component has a triplet fine structure due to coupling with the neighbouring CH_2 groups, with a coupling constant of around 8 Hz (Table 2). Two such triplet of doublet patterns are observed for **2e**. It appears that in this case, the differing neighbourhood relations caused by the diastereoisomerism of the compounds **2** becomes significant: while the ratio in which the two diastereomers are formed is 1:3 under statistical control (see above), the individual neighbourhood relations, seen by a phosphorus-bound proton in the *RRR/SSS* diastereomer are all the same (Figure 2).

Figure 2. Protonic interactions in the two diastereomers of **2e**

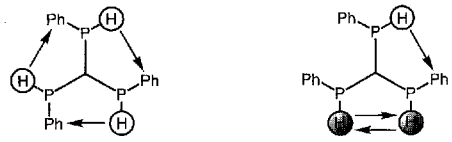

RRR/SSS-Diastereomer *RRS/SSR*-Diastereomer

In the *RRS/SSR* diastereomer, the environment of each of the three PH groups is different (Figure 2). Only one of the protons resides in an immediate environment equivalent to that which surrounds the protons in the *RRR/SSS* diastereomer (Figure 2). The other two phosphorus-bound protons have different but closely similar environments (Figure 2). It is assumed that these two protons lead to one of the equally intense multiplet structures seen for **2e**. The

intensity expected for this signal is thus 2 × 3/4, corresponding to the presence of two protons of this environment in the major diastereomer *RRS/SSR*, which corresponds to three-quarters of the total. The intensity of the signal corresponding to the remaining four protons corresponds to 3 × 1/4 plus 1 × 3/4, with respect to the three equivalent protons in the diastereomer making up only one-quarter of the total and the one proton in the major diastereomer making up three-quarters of the total. The signals should thus be of equal intensity, as is indeed observed (Table 2).

The ^{13}C-NMR spectra (Table 2) show the expected signals for the compounds **2** in each case. The ^{31}P-NMR spectra (Table 3) reveal the presence of the two diastereomeric forms of **2** in the expected ratio of 1:3 for the signals corresponding to the homochiral species (*RRR/SSS*) relative to the signals of the *RRS/SSR* diastereomer. The homochiral diastereomer gives rise to just one singlet (Table 3). For the other diastereomer, where the environment of each of the phosphorus nuclei is different, a doublet of doublet structure is at the extreme of what one might expect for each individual phosphorus nucleus in this diastereomer (Table 3). This structure is found to collapse to produce either a pseudo triplet (**2c, e**) or even a doublet (**2b**) or a multiplet (**2d**) (Table 3.).

Table 2. ^1H- and ^{13}C-NMR data of compounds **2**[a]

No.	^1H NMR δ	^{13}C NMR δ
2b	1.32 [s, 3 H, CH_3C_q], 1.81–2.10, 2.21–2.66 [m, 6 H, CH_2P], 2.41 [s, 9 H, Aryl–CH_3], 4.20 [td, $^1J_{HP}$ = 210 Hz, $^3J_{HH}$ = 8 Hz, 3 H, PH], 7.18–7.71 [m, 12 H, aromatic H]	21.8 [s, Aryl–CH_3], 28.8 [m, CH_3C_q], 37.9 [m, CH_2P, C_q], 129.5–138.7 [m, aromatic C]
2c	1.36 [s, 3 H, CH_3C_q], 1.61–2.05, 2.42–2.71 [m, 6 H, CH_2P], 2.54 [s, 9 H, Aryl–CH_3], 4.14 [td, $^1J_{HP}$ = 212 Hz, $^3J_{HH}$ = 9 Hz, 3 H, PH], 7.16–7.58 [m, 12 H, aromatic H]	22.2 [d, $^3J_{CP}$ = 14 Hz, Aryl–CH_3], 28.5 [m, CH_3C_q], 36.0 [m, CH_2P], 37.9 [m, C_q], 126.5–135.1 [m, aromatic C]
2d	1.30 [s, 3 H, CH_3C_q], 1.62–2.04, 2.40–2.69 [m, 6 H, CH_2P], 2.37 [s, 18 H, Aryl–CH_3], 4.10 [td, $^1J_{HP}$ = 206 Hz, $^3J_{HH}$ = 8 Hz, 3 H, PH], 7.20–7.60 [m, 9 H, aromatic H]	21.7 [m, Aryl–CH_3], 28.7 [m, CH_3C_q], 37.7 [m, CH_2P, C_q], 130.5–138.4 [m, aromatic C]
2e	1.69–1.94, 2.36–2.64 [m, 6 H, CH_2P], 2.98 [s, 2 H, $PhCH_2$], 4.22, 4.26 [td, $^1J_{HP}$ = 210 Hz, $^3J_{HH}$ = 8 Hz, 1.5 H, PH], 7.26–7.74 [m, 20 H, aromatic H]	35.0 [m, CH_2P], 41.8 [m, $PhCH_2$], 45.1 [m, C_q], 126.1–129.0 [m, aromatic C]

[a] Solvent: $CDCl_3$; C_q ≡ quaternary C.

The tripod ligands **2** react with $(CH_3CN)_3Mo(CO)_3$[12] to produce the tricarbonyl molybdenum derivatives **3** (Figure 3). The synthesis and properties of compound **3a** have been described previously[11]. The properties of **3b–e** are similar to those reported for **3a**[11]. Compounds **3** are obtained as microcrystalline solids; they are light-yellow in colour, but may appear light-brown to light-green, even in an analytically pure state, presumably due to very slight contamination by intensely coloured decomposition products.

Table 3. ^{31}P-NMR data of compounds **2**[a]

No.	*RRR/SSS* [b]	*RRS/SSR* [b]		
	$\delta(^{31}P)$	$\delta_1(^{31}P)$	$\delta_2(^{31}P)$	$\delta_3(^{31}P)$
		$^4J_{12}$ (Hz)	$^4J_{23}$ (Hz)	$^4J_{13}$ (Hz)
2b	–71.90 (s)	–72.35 (d, bs)		–72.70 (pt)
		8.0		8.0
2c	–78.70 (s)	–79.36 (pt)	–79.50 (pt)	–80.10 (pt)
		4.9	4.9	4.9
2d	–70.69 (s)	–70.96–(–71.19) (m)		–71.47 (pt)
		5.3		5.3
2e	–71.40 (s)	–71.93 (pt)	–72.18 (pt)	–72.93 (pt)
		7.0	7.0	7.0

[a] Solvent: $CDCl_3$. – [b] *RRR/SSS* and *RRS/SSR* characterize the diastereomers of **2** by indicating the configuration (*R* or *S*) at the phosphorus atoms. The integrated intensity for the signal of the *RRR/SSS* diastereomer is one-third of the pattern observed for the *RRS/SSR* isomer. δ_i is the chemical shift of the phosphorus centre *i* (*i* = 1, 2, 3). *J* denotes coupling constants in hertz.

Figure 3. Preparation of compounds **3**

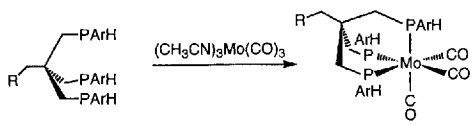

2 **3**

Nr.	R	Ar
2a, 3a	H	Ph
2b, 3b	H	4-MeC_6H_4
2c, 3c	H	2-MeC_6H_4
2d, 3d	H	3,5-$Me_2C_6H_3$
2e, 3e	Ph	Ph

Characteristic mass spectra (Table 4), indicating the consecutive loss of up to three CO groups and IR spectra showing the typical two band pattern of the $Mo(CO)_3$ groups (Table 4) are in themselves almost conclusive as to the composition of compounds **3**.

Table 4. MS (EI) and IR data of compounds **2**

No.	(*m/z*) (%)	(*m/z*) (%)	(*m/z*) (%)	(*m/z*) (%)	IR (CH_2Cl_2) $\tilde{\nu}_{CO}$ [a] (cm^{-1})
3b	620 (41)	592 (14)	562 (54)	534 (100)	1941 (vs)
	[M^+]	[M^+ – CO]	[M^+ – 2CO, – 2H]	[M^+ – 3CO, – 2H]	1845 (vs)
3c	620 (18)	592 (8)	564 (18)	534 (44)	1943 (vs)
	[M^+]	[M^+ · CO]	[M^+ – 2CO]	[M^+ – 3CO, – 2H]	1853 (vs)
3d	660 (28)	632 (8)	604 (52)	576 (100)	1942 (vs)
	[M^+]	[M^+ · CO]	[M^+ – 2CO]	[M^+ – 3CO]	1848 (vs)
3e	654 (37)	626 (18)	596 (60)	568 (100)	1946 (vs)
	[M^+]	[M^+ – CO]	[M^+ – 2CO, – 2H]	[M^+ – 3CO, – 2H]	1854 (vs)

[a] Local C_{3v} symmetry.

As the ligands **2** are obtained in a statistical 1:3 ratio of the *RRR/SSS* versus the *RRS/SSR* diastereomers, the same ratio is observed for the two diastereomeric forms of their coordination compounds **3**: the *RRR/SSS* diastereomer, having three equivalent phosphorus nuclei, gives rise to one singlet in the ^{31}P-NMR spectrum of a compound of type **3** (Table 5). For the three different phosphorus nuclei in the *RRS/SSR* diastereomer, individual signals are observed in each case (Table 5). Due to the coordination, a new coupling pathway is established between these nuclei, producing an increased $^2J_{PP}$ coupling constant relative to the $^4J_{PP}$

coupling constant apparent for the free ligands **2** (Tables 3 and 5). A doublet of doublet structure of the individual signals is observed for each of the compounds **3** (Table 5). These observations are thus similar to those reported previously for compounds of the general type $\{H_3CC-[CH_2P(Ph)(R)]_3\}Mo(CO)_3$[11].

Table 5. ^{31}P-NMR data of compounds **3**[a]

No.	*RRR/SSS* [b]		*RRS/SSR* [b]	
	$\delta(^{31}P)$	$\delta_1(^{31}P)$	$\delta_2(^{31}P)$	$\delta_3(^{31}P)$
		$^2J_{12}$ (Hz)	$^2J_{23}$ (Hz)	$^2J_{13}$ (Hz)
3b	−16.90	−12.55	−14.35	−20.20
		(dd)	(dd)	(dd)
		18	32	32
3c	−30.79	−26.57	−28.91	−33.31
		(dd)	(dd)	(dd)
		19.0	34.8	31.3
3d	−15.91	−11.25	−13.30	−19.93
		(dd)	(dd)	(dd)
		20.5	37.7	31.9
3e	−16.27	−12.12		−20.00
		(dd)	14.82 (dd)	(dd)
		18.2	38.5	32.4

[a] Solvent: $CDCl_3$. – [b] *RRR/SSS* and *RRS/SSR* characterize the diastereomers of **3** by indicating the configuration (*R* or *S*) at the phosphorus atoms. The integrated intensity for the signal of the *RRR/SSS* diastereomer is one-third of the pattern observed for the *RRS/SSR* isomer. δ_i is the chemical shift of the phosphorus centre *i* (*i* = 1, 2, 3). *J* denotes coupling constants in hertz.

Generally speaking, the ^{1}H-NMR spectra of **3** are not adequately resolved at 200 MHz (Table 6). The expected ratio for the chemically different groups is however observed in each case. The signals of the phosphorus-bound protons, being split into many components by phosphorus as well as by hydrogen coupling could not be assigned at the available resolution, even with phosphorus decoupling (Table 6). The signals cannot be unequivocally detected and are thus presumably hidden by the prevailing multiplets of the organic residues. The ^{13}C-NMR spectra (Table 6) are fully consistent with the assigned constitutions of compounds **3**.

Table 6. ^{1}H- and ^{13}C-NMR data of compounds **3**[a]

No.	^{1}H NMR δ	^{13}C NMR δ
3b	0.5–2.9 [m, 18 H, $C\underline{H}_3$, $C\underline{H}_2$], 6.86–7.65 [m, 12 H, aromatic H]	21.6 [s, Aryl–CH_3], 33.6 [s, $\underline{C}H_3C_q$], 37.3 [m, C_q], 39.3 [m, CH_2P], 129.1–133.3 [m, aromatic C], 219.8 [m, CO]
3c	0.6–2.9 [m, 18 H, $C\underline{H}_3$, $C\underline{H}_2$], 6.7–7.9 [m, 12 H, aromatic H]	22.5 [s, Aryl–CH_3], 32.0 [s, $\underline{C}H_3C_q$], 37.5 [m, C_q], 39.7 [m, CH_2P], 124.8–132.6 [m, aromatic C], 216.7 [m, CO]
3d	0.6–2.6 [m, 27 H, $C\underline{H}_3$, $C\underline{H}_2$], 6.84–7.41 [m, 9 H, aromatic H]	21.7 [s, Aryl–CH_3], 33.6 [m, $\underline{C}H_3C_q$], 37.2 [m, C_q], 39.3 [m, CH_2P], 129.3–132.1 [m, aromatic C], 222.4 [m, CO]
3e	0.8–2.8 [m, 8 H, CH_2], 7.1–7.7 [m, 20 H, aromatic H]	31.0 [m, CH_2P], 40.8 [m, $Ph\underline{C}H_2$], 42.6 [m, C_q], 56.1 [m, $PhCH_2C_q$], 127.5–133.1 [m, aromatic C], 220.4 [m, CO]

[a] Solvent: $CDCl_3$; C_q ≡ quaternary C.

In order to test the hypothesis that the ligands coordinated in **3** may be deprotonated at all three PH functions, a THF solution of **3a** was treated with three equivalents of MeLi (Figure 4, route B). Immediate reaction with evolution of methane was observed. Addition of further MeLi did not result in any further gas evolution. The deprotonation may thus be conducted as a form of titration. The trilithio species **4** form red THF solutions.

Figure 4. The two routes to the trilithio species **4**

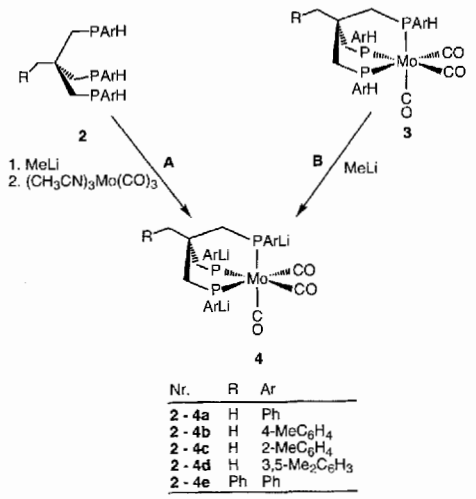

Nr.	R	Ar
2 - 4a	H	Ph
2 - 4b	H	4-MeC_6H_4
2 - 4c	H	2-MeC_6H_4
2 - 4d	H	3,5-$Me_2C_6H_3$
2 - 4e	Ph	Ph

The ν(CO) IR spectra of the solutions (e.g. **4a** 1947 cm^{-1}, 1910 cm^{-1}, 1869 cm^{-1}, 1817 cm^{-1}) show the expected low-frequency shift relative to the corresponding bands of **3a** (1945 cm^{-1}, 1853 cm^{-1})[11]. These four ν(CO) bands for the trilithio derivative **4a** indicate that there are at least two different types of aggregate present in solution. There appears to be a dynamic exchange between these different types of aggregates, since neither ^{1}H- nor ^{31}P-signals are observed for the solution at 20°C. At −30°C, the ^{31}P-NMR spectrum consists of a multitude of signals in the range δ = +9 and δ = −17, thus indicating the coexistence of several types of aggregates. ^{7}Li spectra may be obtained at 20°C. These feature broad, fine-structured signals at δ = 1. All these observations taken together indicate that there are several ways in which the three phosphido groups in **4** may associate with their lithium counterions and the THF solvent. This interpretation is corroborated by the observation that upon addition of [2,2,2]-cryptand, the THF solution of **4a** shows only two ν(CO) bands (1915 cm^{-1}, 1832 cm^{-1}), as expected for $\{H_3CC[CH_2P(Ph)]_3Mo(CO)_3\}^{3-}$.

The trilithiotriphosphido coordination compounds **4** may also be obtained by direct substitution of the CH_3CN groups in $(CH_3CN)_3Mo(CO)_3$ by the trilithio derivatives of **2** in THF (Figure 4). This was exemplified by the corresponding transformation of **2a** into **4a**: the trilithio derivative of **2a**, prepared from **2a** by titration with MeLi in THF, reacts with $(CH_3CN)_3Mo(CO)_3$ to produce a solution of **4a**. The THF solutions of **4a** thus obtained are identical to the solutions of **4a** prepared by deprotonation of **3a** (see above) in all their properties.

THF solutions of **4** leave a brown solid material after evaporation of the solvent. This material is self-igniting in air; it may be redissolved in THF giving solutions with all the properties characteristic of the solutions of **4** described

above. In the case of **4a**, it has been shown that treatment of the solution with HBF4·Et2O gives the starting compound **3a** (Figure 5). No diastereomeric discrimination is observed in this case since the 1:3 ratio of the *RRR/SSS* versus the *RRS/SSR* diastereomer, observed for the starting material (see above), remains unchanged throughout the transformation of **3a** to **4a** and of **4a** back to **3a** (Figure 5) by acidification.

Figure 5. Preparation of **4a**

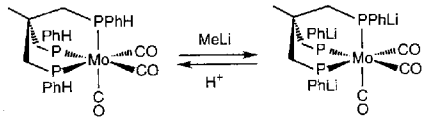

3a **4a**

While diastereomeric differentiation is not observed when compounds **4** are treated with protons as the electrophilic agents, such a differentiation is observed when organic electrophiles are used instead. Compounds **5a–d** are obtained by treating solutions of **4** with MeI, EtBr, *i*PrCl and BzlCl, respectively, as the electrophiles. These derivatives were found to be identical in all their scalar properties to authentic samples of the same species that had been obtained previously by the reaction of the preformed ligands $H_3CC[CH_2P(Ph)(R)]_3$ with $(CH_3CN)_3Mo(CO)_3$[11].

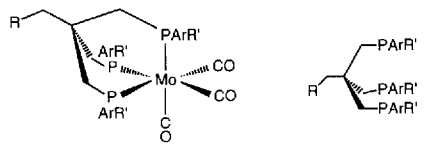

5 **6**

Table 7. Diastereomeric ratios for the formation of compounds **5** and **6**[a]

No. 5, 6	R	Ar	R'	diastereomeric ratio *RRR/SSS* : *RRS/SSR*	diastereomeric ratio *RRR/SSS* : *RRS/SSR*
a	Me	Ph	Me	1:1[a]	0.3:1[b]
b	Me	Ph	Et	0.6:1[a]	0.3:1[b]
c	Me	Ph	*i*Pr	0.3:1[a]	0.3:1[b]
d	Me	Ph	CH_2Ph	2.2:1[a]	only *RRS/SSR*
e	Me	Ph	$CH_2(2,5\text{-}Me_2C_6H_3)$	2:1[a]	0.2:1[a]
f	Me	Ph	CH_2(2-naph.)	4:1[a]	0.3:1[b]
g	Me	4-MeC_6H_4	CH_2Ph	1.3:1[a]	0.3:1[a]
h	Me	2-MeC_6H_4	CH_2Ph	2:1[b]	– [d]
i	Me	$3,5\text{-}Me_2C_6H_3$	Me	0.8:1[a]	0.3:1[b]
j	Me	$3,5\text{-}Me_2C_6H_3$	Et	0.5:1[b]	0.3:1[b]
k	Me	$3,5\text{-}Me_2C_6H_3$	CH_2Ph	2.1:1[b]	0.4:1[b]
l	Ph	Ph	CH_2Ph	4.1:1[b]	0.3:1[b]

[a] Diastereomeric ratio determined by simulation of the ^{31}P-NMR spectra. – [b] Signal shape and resolution allowed for direct integration of the ^{31}P-NMR spectra. – [c] Diastereomeric ratios of the ligands **6** were determined by transforming them into their $Mo(CO)_3$ derivatives of type **5** and integrating or simulating the ^{31}P-NMR spectra. Statistical ratio *RRR/SSS* : *RRS/SSR* = 1:3. – [d] Resolution of the ^{31}P-NMR spectra is not sufficient for simulation or integration.

There is however one important difference: the diastereomeric ratio in which the two enantiomeric pairs *RRR/SSS* and *RRS/SSR* are formed differs markedly from the statistical ratio of 1:3 (Table 7). The formation of the homochiral pair (*RRR/SSS*) is significantly preferred, except in the case with *i*PrCl as the electrophile (**5c**) (Table 7). When the ligands are prepared by treating the trilithiotriphosphide $H_3CC[CH_2P(Ph)(Li)]_3$ with organic electrophiles, the only case where diastereomeric discrimination is observed is that employing BzlCl as the electrophile[11]. In this case, however, a strong bias towards the *RRS/SSR* pair had been observed, resulting in an almost exclusive formation of this diastereomer. In marked contrast, reaction of the coordinated triphosphide **4a** with BzlCl leads to a considerable excess of the homochiral (*RRR/SSS*) racemate (**5d**) (Table 7). In this case, the diastereomer which would be expected to be the minor component on statistical grounds is in fact the major product.

The diastereomeric ratio in which the diastereomers of **5a–d** are obtained is not dependent on the way (route A or B, Figure 4) in which the trilithiotriphosphide precursor **4** is formed. This result was obtained by producing the trilithiotriphosphide-$Mo(CO)_3$ precursor $\{H_3CC[CH_2P(Ph)(Li)]_3\}Mo(CO)_3$ via both routes (routes A and B, Figure 4) and reacting the respective products with MeI, EtBr, *i*PrCl and BzlCl. The same diastereomeric mixture of **5a–d** was obtained irrespective of the nature of the formation step. This is an additional proof for the statement made earlier that the compounds prepared following either route A or B (Figure 4) are identical.

In order to find out whether the diastereomeric differentiation observed, which is especially strong with BzlCl as the electrophile, is sensitive to the bulkiness of the aryl group in RCH_2Cl, **5e** and **5f** were synthesized starting from **4** and $ClCH_2(2,5\text{-}Me_2C_6H_3)$ (**5e**) and $BrCH_2$(2-naph.) (**5f**), respectively. To probe the steric influence of the Phenyl substituents at the triphosphide nucleophile, compounds **5g–k** were prepared from the corresponding $\{H_3CC[CH_2P(Ar)(Li)]_3\}Mo(CO)_3$ precursors. The influence of a sterically more demanding group at the backside of the chelate cage was studied using $\{PhCH_2C[CH_2P(Ar)(Li)]_3\}Mo(CO)_3$ as the precursor (**5l**). The dependence of the diastereomeric ratio on the reaction conditions was analysed as follows by using $\{H_3CC[CH_2P(Ph)(Li)]_3\}Mo(CO)_3$ as the standard nucleophile and BzlCl as the electrophile: instead of adding the pure electrophile to 5×10^{-2} M THF solutions of the trilithiotriphosphide, a 2×10^{-1} M THF solution of the electrophile was added to a 5×10^{-2} M THF solution of the trilithiotriphosphide under high dilution conditions. Within the limits of error, the diastereomeric ratio obtained in this way was equal to that obtained without applying the dilution principle. The implication of this is that if aggregates are involved in the reaction these should be so stable that they stay uninfluenced by dilution, or more probably that no aggregates are involved in the reaction. When [2,2,2]-cryptand was added to the solution of the triphosphide, the infrared spectra changed as described previously, leading to a two-band pattern as would be expected for an $Mo(CO)_3$ chromophore with essentially C_{3v} symmetry. When BzlCl was added to this solution, no reaction was observed. A probable explanation for this observation is a complete blocking of the

reaction channels that otherwise allow the approach of the electrophile.

The diastereomeric ratios given in Table 7 were determined by ^{31}P-NMR spectroscopy. Since the spectra are generally no longer first-order, the patterns were simulated[14] (Table 10). To facilitate the simulation procedure for **5e–l**, these compounds were also synthesized from $(CH_3CN)_3Mo(CO)_3$ and the free ligands $RCH_2C[CH_2P(Ar)(R)]_3$ (**6**). The ligands themselves were obtained from compounds **2** by titration with MeLi in THF and subsequent addition of the appropriate electrophile. Upon synthesizing **5** via this route, the diastereomeric ratio corresponds to that obtained during the preparation of the ligand. This ratio is close to the statistical ratio of *RRR/SSS* to *RRS/SSR* of 1:3 for all the ligands in **5e–l** and the exclusive formation of the *RRS/SSR* diastereomer during the synthesis of the ligand present in **5d**[11] appears to be a solitary exception. The ^{31}P-NMR spectra of the diastereomeric mixtures thus obtained are easier to simulate because the intensity of the manifold of signals due to the *RRS/SSR* diastereomer is enhanced by a factor of up to twelve (**5l**, Table 7) compared to the singlet signal of the *RRR/SSS* isomer. As an example, the experimental and simulated spectra of **5e** are given in Figure 6.

The ^{31}P-NMR data for **5e–l** are given in Table 8. They are characterized by rather small differences in the chemical shift values of the chemically different phosphorus centers and $^2J_{PP}$ coupling constants of around 15–29 Hz (Table 8). The ^{31}P-NMR spectrum of **5h**, with an *o*-tolyl group bound to each of the phosphorus atoms, could not be simulated this way. Presumably, owing to the different orientations of the *o*-tolyl groups in the compound, the signals are broad and are not sufficiently resolved. The resolution obtained with a 200 MHz spectrometer is also insufficient for a complete analysis of the ^{31}P-NMR spectra of **5j**, **k**, **l**. Integration of the different groups of signals nevertheless allows for the evaluation of the diastereomeric ratios (Table 7). The numbers given for the ratios as determined from simulation experiments are reproducible to within ±0.1. The data obtained by integration are less accurate, approximately ±0.3.

The ^{1}H-NMR spectra of compounds **5** are less useful for determining the diastereomeric ratio. There are too many overlapping signals to allow unambiguous resolution of one-dimensional 200 MHz NMR spectra (Table 9). Nevertheless, the spectra are conclusive as to the constitution of the compounds, even in cases where the signals of a number of different groups overlap to a large extent (**5i**, **j**, Table 9). The signals of the aryl residues in the CH_2 substituents of

Figure 6. Experimental and simulated ^{31}P-NMR spectra of **5e** (A: **5e** prepared from the coordinated ligand precursor **4a**, experimental spectrum below, simulated above; B: **5e** prepared from the free ligand **2a**, experimental spectrum below, simulated above). A shows the spectrum of a sample of **5e** as obtained from the preformed ligand. The diastereomeric ratio *RRR/SSS* versus *RRS/SSR* is 0.2 : 1 in this case, while it is 2:1 when **5e** is prepared from the coordinated ligand precursor (**B**)

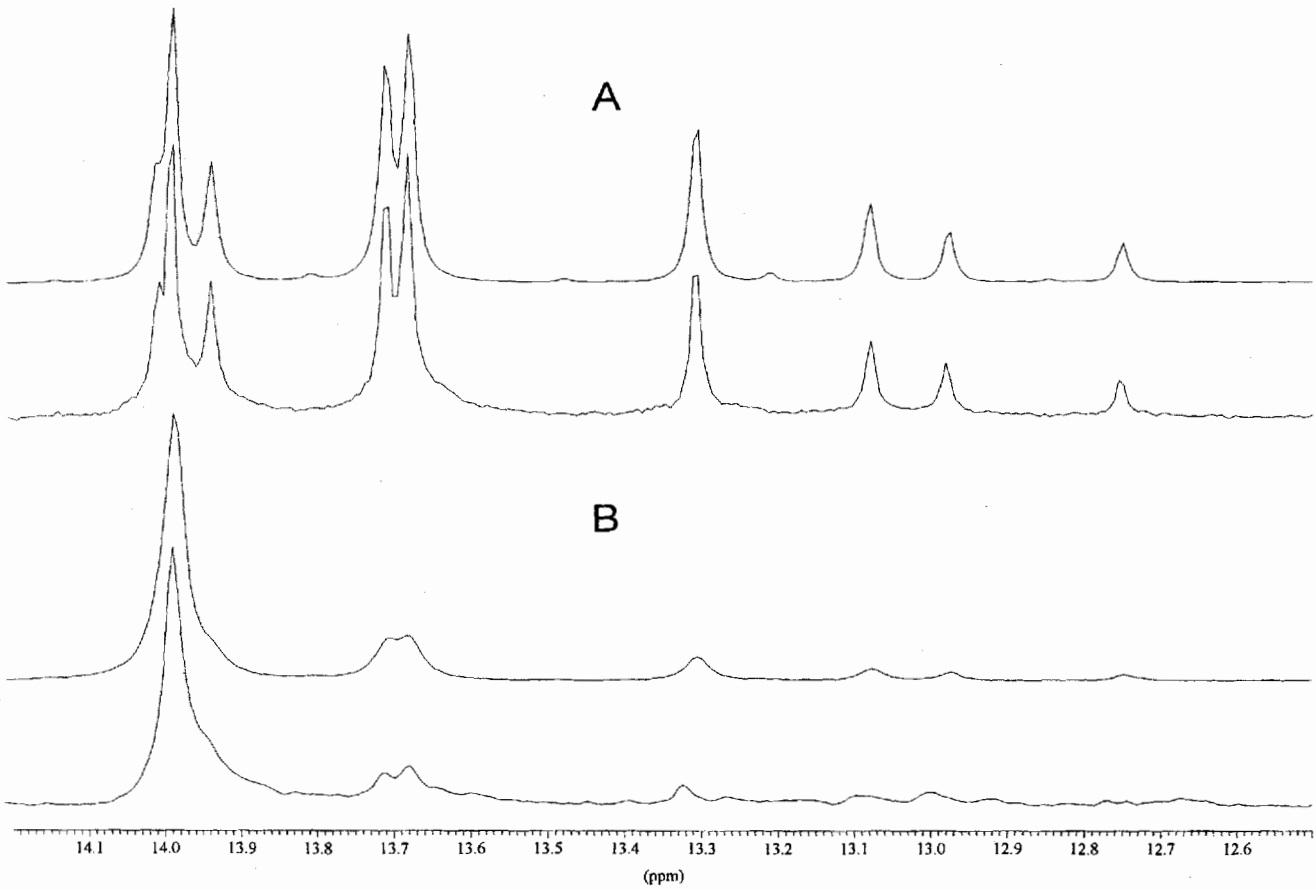

5d–h and **5k, l** are in part resolved and are characteristic of these aryl groups. The spectrum of **5e** could be resolved by two-dimensional (COSY) spectroscopy (Table 9). Both samples of **5e**, the one prepared from the coordinated precursor with the diastereomeric ratio of 2:1 (Table 7) and the one synthesized from the preformed ligand **6e** showing a diastereomeric ratio of 0.2 : 1 (Table 7), were analysed. This analysis allowed the assignment of a number of signals corresponding to just one of the two diastereomers. These signals are correspondingly designated in Table 10. The integral ratios given were scaled such that the sum of the integrals corresponding to equivalent groups in the two diastereomers added up to the number of protons belonging to these groups. The diastereomeric ratio as determined from this experiment is again 2:1, thus corresponding to that determined by ^{31}P-NMR spectroscopy (Table 7).

Table 8. ^{1}H-NMR data of the diastereomeric mixture of **5** as obtained from $\{RCH_2C[CH_2P(Ar)(Li)]_3\}Mo(CO)_3$[a]

No.	*RRR/SSS* [b]		*RRS/SSR* [b]	
	$\delta(^{31}P)$	$\delta_1(^{31}P)$	$\delta_2(^{31}P)$	$\delta_3(^{31}P)$
		$^2J_{12}$ (Hz)	$^2J_{23}$ (Hz)	$^2J_{13}$ (Hz)
5e	14.00 (s)	13.08 (dd)	13.80 (dd)	13.82 (dd)
		27	15	20
5f	13.88 (s)	13.74 (dd)	14.43 (dd)	14.99 (dd)
		27.5	24.7	25.9
5g	12.43 (s)	12.06 (dd)	12.42 (dd)	13.35 (dd)
		25	16	28
5h	7.2 (s)		7.0–8.7 (m)	
5i	3.61 (s)	2.19 (dd)	2.21 (dd)	3.06 (dd)
		21	29	21
5j	13.7 (s)		13.9–14.4 (m)	
5k	12.20 (s)	11.76 (dd)	12.73 (dd)	13.57 (dd)
		26.1	23.1	28.0
5l	10.73 (s)	11.21 (dd)	11.51 (dd)	12.85 (dd)
		23	18	29

[a] Solvent: $CDCl_3$.

The observation regarding the ratio in which the two diastereomeric forms of the ligands **6** are obtained, depending on whether they are prepared from the free ligand precursors $RCH_2C[CH_2P(Ar)(Li)]_3$ or from the coordinated compounds $\{RCH_2C[CH_2P(Ar)(Li)]_3\}Mo(CO)_3$, merits some comment. It is evident that with the free ligand precursors this ratio is close to the statistical one of 0.33 (*RRR/SSS* / *RRS/SSR*), with the single exception of $H_3CC[CH_2P(Ph)(Bzl)]_3$, where a strong bias towards the preferred formation of the *RRS/SSR* diastereomer had been observed[11] (Table 7). On the other hand, when the ligands **6** are formed from the appropriate η^3-coordinated precursors in their $Mo(CO)_3$ derivatives **5**, a strong bias towards the formation of the statistically less probable *RRR/SSS* diastereomer is observed (Table 7). The only exception in this case is **5c**, where a diastereomeric ratio as expected on statistical grounds is obtained (Table 7). The diastereomeric ratio obtained depends on the incoming electrophile, as well as on the nature of the phosphido-bound aryl group (Table 7). A clear trend is only apparent for the dependence of the nature of the incoming electrophile: benzylic electrophiles (**5d–h**, **5k**, **l**) give higher diastereomeric ratios (Table 7) as compared to alicyclic electrophiles (**5a–c**, **5i**, **j**) (Table 7). This situation remains unchanged when the precursor molecules bear sterically more demanding 2-methyl- (**5h**), 4-methyl- (**5g**) or 3,5-dimethyl- (**5i-k**) phenyl residues rather than simple P–phenyl substituents. It appears that a possible stacking of the phosphorus-bound aryl groups may already be present in the precursors and that the aryl groups introduced by benzylic electrophiles might help to transfer the chiral information from one phosphorus centre to the others. Alkyl groups would clearly be less efficient in such a role. The preferred formation of the *RRR/SSS* diastereomer, which is statistically less probable, must mean

Table 9. ^{1}H-NMR data of the *RRR/SSS* isomer of **5e**[a]

No.	^{1}H NMR	
	CH, CH_2, CH_3 δ	aromatic H δ
5e	1.16 [s, 2.4 H, *o*-Aryl–CH_3]	5.71 [s, 1 H]
	1.19 [s, 1.8 H, *o*-Aryl–CH_3]	5.98 [s, 1 H]
	1.64, 1.67 [s, 2.4 H, *o*-Aryl-CH_3]	6.60 [s, 1 H]
	2.09 [s, 4.2 H, *m*-Aryl–CH_3]	6.64–7.79 [m, 21 H]
	2.27, 2.31 [s, 2.4 H, *m*-Aryl–CH_3]	
	1.2–2.47 [m, 9.6 H, CH_3C_q, CH_2C_q, CH_2(2,5-$Me_2C_6H_3$)]	
	2.56–3.76 [m, 5.4 H, CH_2(2,5-$Me_2C_6H_3$)]	
5f	1.20 [s, 3 H, CH_3C_q]	6.09 [d, J_{HH} = 8.3 Hz, 1 H]
	1.29–2.00 [m, 6 H, CH_2C_q]	6.33 [d, J_{HH} = 8.5 Hz, 1 H]
	2.62 [dd, $^2J_{HH}$ = 14.4 Hz, $^2J_{HP}$ = 3.7 Hz, 1 H, C_1HH_a(2-naph.)]	6.64 [d, J_{HH} = 8.0 Hz, 1 H]
		6.78 [d, J_{HH} = 8.3 Hz, 1 H]
	3.09 [dd, $^2J_{HH}$ = 14.4 Hz, $^2J_{HP}$ = 3.6 Hz, 1 H, C_1HH_b(2-naph.)]	6.99–7.94 [m, 32 H]
	3.26–3.92 [m, 4 H, CH_2(2-naph.)]	
5g	1.28 [s, 3 H, CH_3C_q]	6.03 [s, 2 H]
	1.62–1.93 [m, 6 H, CH_2C_q]	6.50 [d, J_{HH} = 3.9 Hz, 2 H]
	2.37–2.43 [m, 9 H, Aryl–CH_3]	6.75 [d, J_{HH} = 7.6 Hz, 2 H]
	2.87–3.64 [m, 6 H, CH_2Ph]	6.83–7.88 [m, 21 H]
5h	1.34 [s, 3 H, CH_3C_q]	6.18 [s, 2 H]
	1.46–2.03 [m, 6 H, CH_2C_q]	6.54 [s, 2 H]
	2.38–4.17 [m, 15 H, CH_2Ph, Aryl–CH_3]	6.65 [d, J_{HH} = 5.3 Hz, 2 H]
		6.87–7.48 [m, 21 H]
5i	1.30 [s, 3 H, CH_3C_q]	6.88–7.53 [m, 9 H]
	0.7–2.4 [m, 30 H, CH_3P, CH_2P, Aryl-CH_3]	
5j	1.35 [s, 3 H, CH_3C_q]	6.83–7.46 [m, 9 H]
	0.6–2.4 [m, 39 H, CH_3CH_2, CH_2, Aryl–CH_3]	
5k	1.27 [s, 3 H, CH_3C_q]	5.99 [pt, J_{HH} = 8.0 Hz, 2 H]
	1.45–1.80 [m, 6 H, CH_2C_q]	6.59 [d, J_{HH} = 10.0 Hz, 2 H]
	2.01–2.42 [m, 19 , Aryl–CH_3, C_1HH_aPh]	6.79 [d, J_{HH} = 10.0 Hz, 2 H]
		6.87–7.38 [m, 18 H]
	2.83 [dd, $^2J_{HH}$ = 14.4 Hz, $^2J_{HP}$ = 3.8 Hz, 1 H, C_1HH_bPh]	
	3.07–3.68 [m, 4 H, CH_2Ph]	
5l	1.34–1.96 [m, 6 H, CH_2C_q]	5.83 [d, J_{HH} = 7.4 Hz, 2 H]
	2.24–3.62 [m, 8 H, CH_2Ph]	6.44 [d, J_{HH} = 7.2 Hz, 2 H]
		6.52 [d, J_{HH} = 7.1 Hz, 2 H]
		6.80–7.85 [m, 29 H]

[a] Solvent: $CDCl_3$.

Table 10. ^{31}P-NMR data of compounds **5**[a]

No.	^{1}H NMR	
	CH, CH_2, CH_3 δ	aromatic H δ
5e	1.19 [s, 9 H, *o*-Aryl–CH_3]	5.71 [s, 3 H]
	2.09 [s, 9 H, *m*-Aryl–CH_3]	6.64–7.79 [m, 21 H]
	1.2–2.4 [m, 9 H, CH_3C_q, CH_2C_q]	
	2.59 [d, $^2J_{HH}$ = 14.6 Hz, 3 H, CHH_a(2,5-$Me_2C_6H_3$)]	
	3.27 [d, $^2J_{HH}$ = 14.6 Hz, 3 H, CHH_b(2,5-$Me_2C_6H_3$)]	

[a] Solvent: $CDCl_3$. – [b] *RRR/SSS* and *RRS/SSR* characterize the diastereomers of **5** by indicating the configuration (*R* or *S*) at the phosphorus atoms. The integrated intensity for the signal of the *RRR/SSS* diastereomer is one-third of the pattern observed for the *RRS/SSR* isomer. δ_i is the chemical shift of the phosphorus centre *i* (*i* = 1, 2, 3). *J* denotes coupling constants in hertz.

that the special arrangement of the intermediates $\{RCH_2C[CH_2P(Ar)(R')][(Ar)(Li)]_2\}Mo(CO)_3$ and $\{RCH_2C[CH_2P(Ar)(Li)][(Ar)(R')]_2\}Mo(CO)_3$ is conducive to making the subsequent substitution step occur with the same sense of chirality as that already fixed in the P(Ar)(R′) groups.

From the result obtained with **5l**, it appears that a sterically demanding group (Bzl) at the backside of the ligand tends to increase the bias towards the formation of the homochiral diastereomer (*cf.* **5d**). This may be rationalized by assuming that the channel through which the electrophile has to approach the phosphorus nucleophile is less open towards the rear of the ligand, so that the incoming electrophile is more strongly influenced by the P(Ar) groups at the frontside.

The special arrangement of the P(Ar)(Bzl) groups in **5** was probed by X-ray analysis of **5d**, **k**, **l**. The high diastereomeric ratios in which the homochiral diastereomer is formed in these cases allowed for separation of the clean enantiomeric mixture (*RRR/SSS*) by crystallization. Analytical data, mass spectra and IR spectra of the pure *RRR/SSS* diastereomers are identical to those obtained for the corresponding diastereomeric mixtures. The NMR data are conclusive as to the purity of the diastereomers (Table 11). Only the signals of the homochiral species are observed.

The structures of the three compounds are quite similar with respect to the coordination geometry, as well as to the torsional arrangement of the different groups relative to the coordination octahedron. The distances and angles would not be expected to be too different in the three compounds and in fact they are quite similar (Table 12).

However, at first glance, it seems astonishing that even the torsion angles are quite similar in all three of the compounds. Figure 7 shows the structure of **5d** in a projection onto the P_3 plane.

It is evident from Figure 7 that the compound has almost C_{3v} symmetry, even including the torsional arrangement of the aryl groups. This torsional arrangement is defined in Table 12 with respect to auxiliary vectors pointing towards the observer (Figures 7–10) and being vertical to the P_3 plane, thus pointing in the direction of the approximate C_3 axes.

Table 11. ^{1}H- and ^{31}P-NMR data of the *RRR/SSS* isomers of **5d**, **k**, **l**[a]

No.	^{1}H NMR		^{31}P NMR
	CH, CH_2, CH_3 δ	aromatic H δ	δ
5d	1.24 [s, 3 H, CH_3]	5.95 [d, $^3J_{HH}$ = 7.2 Hz, 6 H]	16.3 [s]
	1.57 [d, $^2J_{HH}$ = 13 Hz, 3 H, CHH_aC_q]	6.89–7.61 [m, 24 H]	
	1.76 [d, $^2J_{HH}$ = 13 Hz, 3 H, CHH_bC_q]		
	2.38 [d, $^2J_{HH}$ = 14 Hz, 3 H, CHH_aPh]		
	3.13 [d, $^2J_{HH}$ = 14 Hz, 3 H, CHH_bPh]		
5k	1.23 [s, 3 H, CH_3]	5.97 [d, $^3J_{HH}$ = 7.0 Hz, 6 H]	12.2 [s]
	1.46 [d, $^2J_{HH}$ = 15.5 Hz, 3 H, CHH_aC_q]	6.91–7.27 [m, 18 H]	
	1.64 [d, $^2J_{HH}$ = 15.5 Hz, 3 H, CHH_bC_q]		
	2.32–2.39 [m, 21 H, Aryl–CH_3, CHH_aPh]		
	3.11 [d, $^2J_{HH}$ = 14.4 Hz, 3 H, CHH_bPh]		
5l	1.30 [d, $^2J_{HH}$ = 15 Hz, 3 H, $PCHH_aC_q$]	5.78 [d, $^3J_{HH}$ = 7.3 Hz, 6 H]	10.8 [s]
	1.84 [d, $^2J_{HH}$ = 15 Hz, 3 H, $PCHH_bC_q$]	6.74–7.41 [m, 29 H]	
	2.21 [d, $^2J_{HH}$ = 13.9 Hz, 3 H, $PCHH_aPh$]		
	2.57 [d, $^2J_{HH}$ = 12.6 Hz, 1 H, $PhCHH_aC_q$]		
	2.80 [d, $^2J_{HH}$ = 12.6 Hz, 1 H, $PhCHH_bC_q$]		
	3.07 [d, $^2J_{HH}$ = 13.9 Hz, 3 H, $PCHH_bPh$]		

[a] Solvent: $CDCl_3$.

Table 12. Selected bond lengths [pm] and angles [°] of compounds **5d**, **k**, **l**[a]

	5d	**5k**	**5l**
Mo–P1	250.5 (3)	249.8 (4)	250.4 (4)
Mo–P2	251.1 (3)	249.3 (3)	249.9 (4)
Mo–P3	251.9 (3)	251.3 (3)	252.1 (4)
Mo–C80	198 (1)	198 (1)	201 (2)
Mo–C81	197 (1)	198 (1)	202 (2)
Mo–C82	199 (1)	196 (1)	202 (1)
O1–C80	118 (1)	117 (2)	111 (2)
O2–C81	118 (1)	116 (1)	112 (2)
O3–C82	118 (1)	118 (2)	109 (2)
P1–Mo–P2	85.4 (1)	81.9 (1)	82.8 (1)
P1–Mo–P3	81.7 (1)	82.2 (1)	83.0 (1)
P2–Mo–P3	81.7 (1)	84.8 (1)	82.0 (1)
C80–Mo–P1	173.8 (3)	172.0 (4)	172.4 (5)
C80–Mo–P2	88.5 (3)	90.1 (4)	90.7 (5)
C80–Mo–P3	98.3 (3)	96.9 (4)	100.1 (5)
C81–Mo–P1	97.4 (3)	96.7 (4)	98.1 (4)
C81–Mo–P2	172.9 (3)	171.7 (3)	172.9 (4)
C81–Mo–P3	92.3 (3)	86.9 (3)	91.1 (4)
C82–Mo–P1	90.4 (4)	89.5 (4)	90.3 (4)
C82–Mo–P2	97.3 (3)	99.6 (4)	98.4 (4)
C82–Mo–P3	172.1 (4)	170.0 (4)	173.2 (4)
Mo–C80–O1	177.1 (9)	178 (1)	178 (1)
Mo–C81–O2	179 (1)	178 (1)	178 (1)
Mo–C82–O3	177 (1)	176 (1)	177 (1)
HzP1–P1–C25–C20	–3.2	8.7	7.4
HzP2–P2–C45–C40	6.4	–0.9	11.1
HzP3–P3–C65–C60	10.2	2.5	0.3
HzC30–C30–C31–C32	–52.7	–58.0	–24.5
HzC50–C50–C51–C52	–65.9	–38.4	–86.3
HzC70–C70–C71–C76	–84.9	–60.5	–59.6

[a] The torsional arrangement of the phosphorus-bound aryl groups is defined with respect to auxiliary vectors HzPX (X = 1, 2, 3) pointing towards the observer (see Figures 7, 9, 10) and being vertical to the P_3 plane. The torsional arrangement of the phosphorus-bound benzyl groups is defined with respect to auxiliary vectors HzCX (X = 30, 50, 70) pointing towards the observer (see Figures 7, 9, 10) and being vertical to the CX (X = 30, 50, 70) plane.

Figure 7. Structure of **5d**

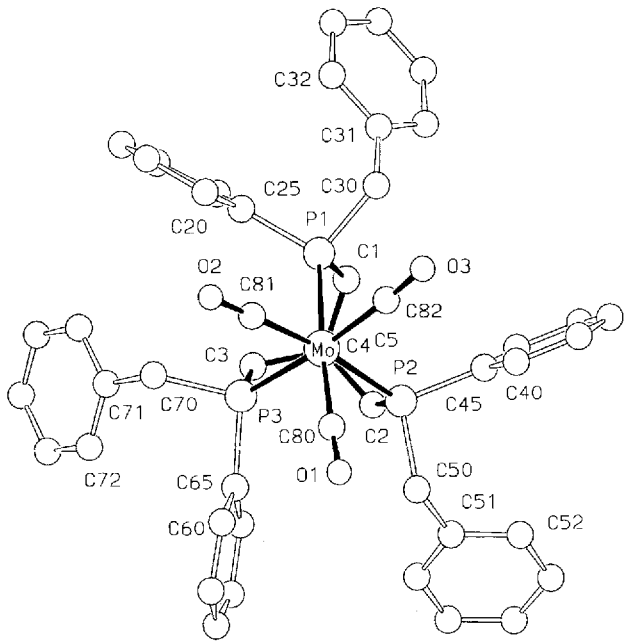

Figure 9. Structure of **5l**

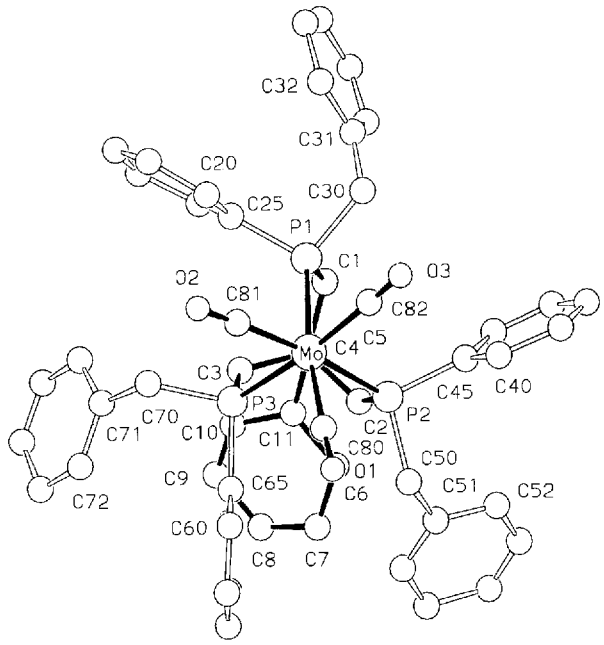

The structures of **5k**, **l** (Figures 8 and 9) are very similar to that observed for **5d** (Figure 7). In order to make the arrangements comparable, the *SSS* enantiomer of **5k** is shown in Figure 8. In the crystal specimen (chiral space group C_2) used for the determination of the structure of **5k**, the compound is present as the *RRR* enantiomer.

Figure 8. Structure of **5k**

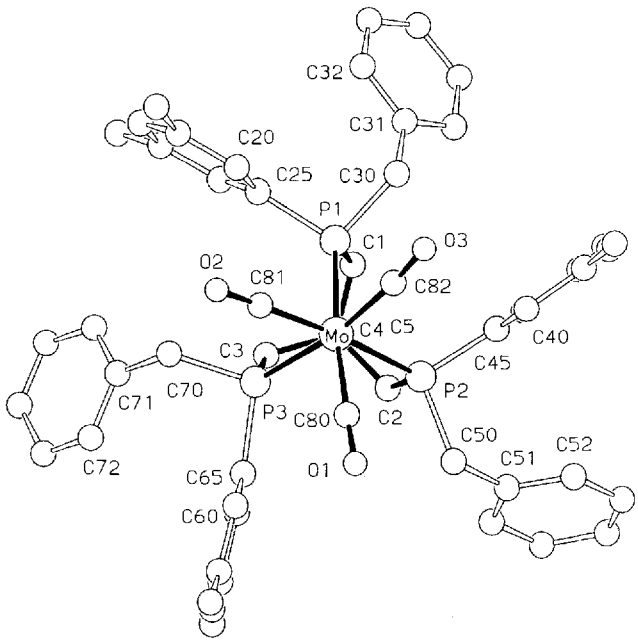

The similarity of the conformation adopted by all the three compounds **5d**, **k**, **l** is even more apparent from Figure 10. To produce this diagram, the coordination octahedra including the three carbonyl groups and the $P_3(CH_2)_3C$-fragment were arranged such that the RMS deviation of the positions of these atoms from each other was minimized[15]. The overlay of the structures of all three compounds **5d**, **k**, **l** (Figure 10) clearly shows that, in spite of three different crystal environments characterizing the solid-state arrangements of the three compounds (Table 22), the conformations adopted by the molecules are astonishingly similar.

Figure 10. Overlay of the structures of **5d**, **k**, **l**

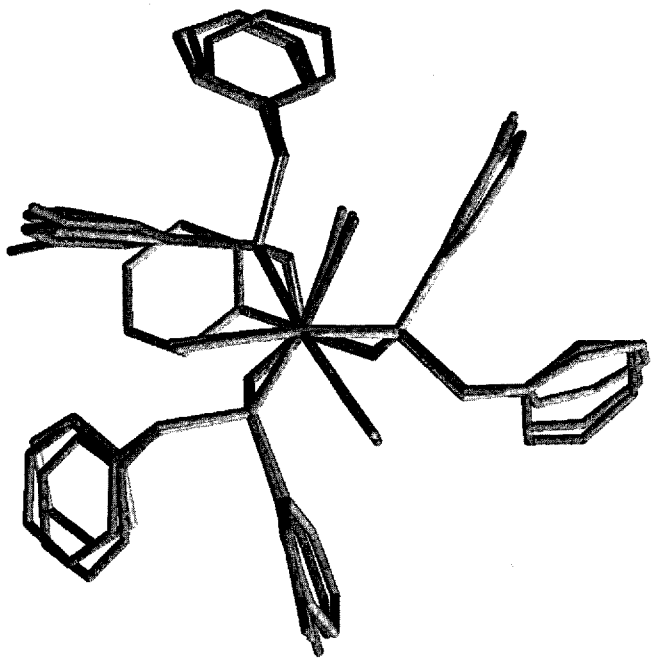

In all three structures, the rotation of the phosphorus-bound aryl groups is such that they are almost parallel to the idealized C_3 (Figures 8–10) axes. The spread of positions occupied by these aryl groups is rather small for the three compounds (Table 12). The rotation of the benzyl

groups is somewhat less restricted, as might be expected with these groups being further away from the center of the compound and being linked to the phosphorus nuclei by two axes of potential rotation ($P-C_{CH2}$, CH_2-C_{aryl}) instead of only one ($P-C_{aryl}$) for the phosphorus-bound aryl groups. Nevertheless, the segment of space occupied by these groups almost coincides for all three of the compounds (Figure 10). What is also evident from Figure 10 is that the Bzl group at the bridgehead carbon of **5l** quite effectively blocks the entrance of one of the three almost equivalent 120° sectors.

Taken together, the similarity of the three structures in the three different compounds, which exist in three different crystal environments (Table 22), suggests that the arrangement observed corresponds to a well-defined minimum of energy resulting from the mutual interaction between aryl and benzyl groups. The high diastereomeric discrimination observed for the formation of **5** with benzyl electrophiles fits into this scheme.

Conclusion

Chiral tripod ligands $RCH_2C[CH_2P(Ar)(R')]_3$ are easily available from $RCH_2C[CH_2P(Ar)_2]_3$. The ratio in which the diastereomers *RRR/SSS* and *RRS/SSR* are formed is generally close to the statistical ratio of 1:3 when the transformation is performed with the non-coordinated ligands[11]. When performed with the ligands coordinated to $Mo(CO)_3$, the equivalent transformation leads to the preferred formation of the *RRR/SSS* diastereomers. This bias towards the formation of the homochiral species must be due to the kinetic control predominating in the cage formed by the η^3-cordination of the ligand to the $Mo(CO)_3$ fragment.

Financial support by the *Deutsche Forschungsgemeinschaft* (DFG, SFB 247), Graduiertenkolleg Chemie, „Selektivität in der Organischen und Metall-Organischen Synthese und Katalyse", the *Stiftung Volkswagenwerk* and the *Fonds der Chemischen Industrie* is gratefully acknowledged. Our thanks are due to *T. Jannack* for mass spectrometry and the people in the microanalytical laboratory of our department for elemental analyses. We thank *D. Günauer* for his help in obtaining CV data.

Experimental Section

General: All manipulations were carried out under an argon atmosphere at 20°C by means of standard Schlenk techniques, unless mentioned otherwise. All solvents were dried by standard methods and distilled under argon. The $CDCl_3$ used for the NMR spectroscopic measurements was degassed by three successive "freeze-pump-thaw" cycles and dried over 4 Å molecular sieves. The silica gel (Kieselgel z.A. 0.06–0.2 mm, J.T. Baker Chemicals B.V.) used for chromatography and the Kieselgur (Kieselgur, washed, heat-treated, Erg. B.6, Riedel de Haen AG) used for the filtration were degassed at 1 mbar at 20°C for 48 h and saturated with argon. – NMR: Bruker Avance DPX 200 at 200.13 MHz (^1H), 50.323 MHz ($^{13}C\{1H\}$), 81.015 MHz ($^{31}P\{1H\}$); chemical shifts (δ) in ppm with respect to $CHCl_3/CDCl_3$ (^1H: δ = 7.27, ^{13}C: δ = 77.0) as internal standards; chemical shifts (δ) in ppm with respect to 85% H_3PO_4 as external standard (^{31}P: δ = 0). – IR: Bruker FT-IR IFS-66; CaF_2 cells. – MS (EI): Finnigan MAT 8400. – Elemental analysis: Microanalytical laboratory of the Organisch-Chemisches Institut, Universität Heidelberg. Under the conditions employed, the carbon-content is often found to be too low for molybdenum-containing compounds due to the formation of non-combustible molybdenum carbide. – Melting points: Gallenkamp MFB-595 010; uncorrected values. – All other chemicals were obtained commercially and used without further purification. – Cyclic voltammetry: Metrohm „Universal Meß- und Titriergefäß" Metrohm GC electrode RDE 628, platinum electrode, SCE electrode, Princeton Applied Research potentiostat Model 273, 10^{-3} M in 0.1 M $n Bu_4NPF_6/CH_2Cl_2$.

Compounds **2**, *$RCH_2C[CH_2P(Ar)(H)]_3$:* To a stirred solution of the ligand **1**[13] (**1b,c**: 7.10 g, 10 mmol; **1d**: 7.91 g, 10 mmol; **1e**: 7.00 g, 10 mmol) in THF (150 ml), small pieces of lithium (1.40 g, 200 mmol) were added. The solution turned deep-red over a period of 10 min. After stirring for 24 h, the lithium was separated by filtration. The red solution was cooled to 0°C and water (50 ml, saturated with nitrogen) was slowly added. The resulting suspension was allowed to warm to room temperature and the aqueous phase was separated. Drying of the organic phase with $MgSO_4$ and subsequent filtration led to a clear, colourless solution. Evaporation of the solvent and drying of the residue in vacuo for 2 d afforded compounds **2** as colourless oils.

Yield: **2b**: 4.30 g (98%); **2c**: 4.25 g (97%); **2d**: 4.71 g (98%); **2e**: 4.63 g (98%).

Table 13. Elemental analyses of **2d** and **2e**[a]

No.	chemical formula	elemental analysis	
2d	$C_{29}H_{39}P_3$	C 68.63 (C 72.48)	H 8.09 (H 8.18)
2e	$C_{29}H_{31}P_3$	C 72.95 (C 73.72)	H 6.79 (H 6.61)

[a] Data in brackets are calculated.

For further experimental data see Tables 1–3.

Compounds **3**, *$\{RCH_2C[CH_2P(Ar)(H)]_3\}Mo(CO)_3$:* To a stirred solution of the ligand **2** (**2b,c**: 880 mg, 2.00 mmol; **2d**: 960 mg, 2.00 mmol; **2e**: 950 mg, 2.00 mmol) in dichloromethane (50 ml), solid $(CH_3CN)_3Mo(CO)_3$[12] (670 mg, 2.20 mmol) was added at 20°C. The solution immediately turned yellow. After stirring for 24 h, the brownish solution was filtered through Kieselgel (4 cm) and Kieselgur (2 cm). The stationary phase was treated with a dichloromethane/petroleum ether (40/60) mixture (ratio 5:1) until the eluent was colourless. Evaporation of the solvent and drying of the residue in vacuo for 2 d afforded compounds **3** as pale-yellow powders.

Yield: **3b**: 870 mg (70%); **3c**: 830 mg (67%); **3d**: 940 mg (71%); **3e**: 1.02 g (78%).

Table 14. Elemental analyses of compounds **3**[a]

No.	chemical formula	elemental analysis	
3b	$C_{29}H_{33}MoO_3P_3$	C 56.26 (C 56.21)	H 5.57 (H 5.36)
3c	$C_{29}H_{33}MoO_3P_3$	C 56.07 (C 56.21)	H 5.47 (H 5.36)
3d	$C_{32}H_{39}MoO_3P_3$	C 56.57 (C 58.19)	H 6.06 (H 5.95)
3e	$C_{32}H_{31}MoO_3P_3$	C 54.96 (C 58.71)	H 4.77 (H 4.78)

[a] Data in brackets are calculated.

For further experimental data see Tables 4–6.

Deprotonation of $\{H_3CC[CH_2P(Ph)(H)]_3\}Mo(CO)_3$ (**3a**); *Protonation of $\{H_3CC[CH_2P(Ph)(Li)]_3\}Mo(CO)_3$* (**4a**): To a stirred

solution of **3a**[12] (580 mg, 1.01 mmol) in THF (50 ml), methyllithium (1.6 M in diethyl ether) (1.90 ml, 3.03 mmol) was slowly added at 0°C. The yellow solution turned deep-red. Evaporation of the solvent left a brown powder, which was redissolved in THF (50 ml). The resulting solution was cooled to 0°C and HBF4·Et2O (54%, 0.43 ml, 3.1 mmol) was slowly added. The mixture was allowed to warm to room temperature, stirred for 2 h, and then the brownish solution was filtered through Kieselgel (4 cm) and Kieselgur (2 cm). The stationary phase was treated with a dichloromethane/petroleum ether (40/60) mixture (ratio 5:1) until the eluent was colourless. Evaporation of the solvent afforded compound **3a** as a yellow powder.

Yield: 420 mg (72%).

Compounds **4**, *$\{RCH_2C[CH_2P(Ar)(Li)]_3\}Mo(CO)_3$*: To a stirred solution of the ligand **2** (**2b**,**c**: 1.10 g, 2.5 mmol; **2d**: 1.20 g, 2.5 mmol; **2e**: 1.18 g, 2.5 mmol) in THF (60 ml), methyllithium (1.6 M in diethyl ether, 4.70 ml, 7.50 mmol) was slowly added at 0°C. The colourless solution turned red. The solution was allowed to warm to room temperature and stirred for 2 h. Solid $(CH_3CN)_3Mo(CO)_3$[14] (790 mg, 2.61 mmol) was then added, resulting in an immediate deep-red colouration. After stirring for a further 2 h, the solvent was removed in vacuo. Compounds **4** were obtained as brownish powders, which tenaciously retain THF.

Table 15. IR data of compounds **4**

No.	IR (THF) $\tilde{\nu}_{CO}$ (cm^{-1})			
4a	1947 (vs)	1910 (vs)	1869 (vs)	1817 (vs)
4b	1942 (vs)	1909 (vs)	1855 (vs)	1816 (vs)
4c	1940 (vs)	1907 (vs)	1868 (vs)	1815 (vs)
4d	1939 (vs)	1908 (vs)	1870 (vs)	1818 (vs)
4e	1945 (vs)	1910 (vs)	1869 (vs)	1816 (vs)

Compounds **5**, *$\{RCH_2C[CH_2P(Ar)(R')]_3\}Mo(CO)_3$*

1. From **4**: To a stirred solution of the ligand **2** (**2a**: 1.00 g, 2.5 mmol; **2b**,**c**: 1.10 g, 2.5 mmol; **2d**: 1.20 g, 2.5 mmol; **2e**: 1.18 g, 2.5 mmol) in THF (60 ml), methyllithium (1.6 M in diethyl ether, 4.70 ml, 7.50 mmol) was slowly added at 0°C. The colourless solution turned red. The solution was allowed to warm to room temperature and then stirred for 2 h. Following the addition of solid $(CH_3CN)_3Mo(CO)_3$[14] (790 mg, 2.61 mmol), the solution immediately became deep-red in colour and was stirred for 20 h. Subsequently, it was cooled to 0°C and the alkyl halide [**5a**, **i**: MeI, 1.10 g, 7.7 mmol; **5b**, **j**: EtBr, 840 mg, 7.7 mmol; **5c**: *i*-PrCl, 600 mg, 7.7 mmol; **5d**, **g**, **h**, **k**, **l**: $ClCH_2Ph$, 970 mg, 7.7 mmol; **5e**: $ClCH_2(2,5\text{-}Me_2C_6H_3)$, 1.19 g, 7.7 mmol; **5f**: $BrCH_2$(2-naph.), 1.70 g, 7.7 mmol] was slowly added. The resulting mixture was allowed to warm to room temperature and stirred for 48 h. Evaporation of the solvent left deep-brown powders, which were dissolved in dichloromethane. The resulting solutions were filtered through Kieselgel (4 cm) and Kieselgur (2 cm). The stationary phase was treated with dichloromethane until the eluent was colourless. Evaporation of the solvent and drying of the residue in vacuo for 1 d afforded compounds **5** as yellow powders. **5d**, **e**, **f**, **h**, **k**, **l** were chromatographed on Kieselgel [20 cm, Ø = 4.5 cm, 20°C; eluent: dichloromethane/petroleum ether (40/60) in the ratio: **5d**: 5:1, R_F = 0.66; **5e**: 1:1, R_F = 0.42; **5f**: 2:1, R_F = 0.25; **5h**: 1:1, R_F = 0.46; **5k**: 1:1, R_F = 0.43; **5l**: 1:1, R_F = 0.54].

Yield: **5a**: 1.01 g (65%); **5b**: 1.13 g (68%); **5c**: 1.04 g (59%); **5d**: 790 mg (33%); **5e**: 330 mg (14%); **5f**: 400 mg (13%); **5g**: 1.54 g (69%); **5h**: 360 mg (16%); **5i**: 1.25 g (71%); **5j**: 1.34 g (72%); **5k**: 320 mg (20%); **5l**: 730 mg (23%).

Table 16. ^{13}C-NMR data of compounds **5**[a]

No.	^{13}C NMR	
	C, CH_2, CH_3 δ	aromatic C δ
5e	20.1 [m, Aryl–CH_3]	127.5–136.6 [m]
	31.5 [m, $\underline{C}H_2C_q$]	
	33.2 [m, $\underline{C}H_3C_q$]	
	37.2 [m, C_q]	
	40.2 [m, $\underline{C}H_2Ph$]	
	222.9 [m, CO]	
5f	30.6 [m, $\underline{C}H_2C_q$]	125.8–137.3 [m]
	36.5 [q, $^2J_{CP}$ = 5.6 Hz, C_q]	
	39.4 [q, $^3J_{CP}$ = 8.9 Hz, $\underline{C}H_3C_q$]	
	44.5 [m, $\underline{C}H_2Ph$]	
	222.4 [m, CO]	
5g	21.6 [m, Aryl–CH_3]	126.4–135.1 [m]
	30.4 [m, $\underline{C}H_2C_q$]	
	37.0 [m, C_q]	
	44.2 [m, $\underline{C}H_2Ph$]	
	222 [m, CO]	
5h	22.6 [m, Aryl–CH_3]	125.2–130.1 [m]
	32.4 [m, $\underline{C}H_2C_q$]	
	37.0 [q, $^2J_{CP}$ = 7.6 Hz, C_q]	
	38.8 [m, $\underline{C}H_3C_q$, $\underline{C}H_2Ph$]	
	222.5 [m, CO]	
5i	21.9 [m, Aryl–CH_3]	127.1–138.7 [m]
	22 [m, $\underline{C}H_2C_q$]	
	39 [m, $\underline{C}H_3C_q$, C_q, $\underline{C}H_3P$]	
	222.3 [m, CO]	
5j	8.3 [d, $^2J_{CP}$ = 7 Hz, $\underline{C}H_3CH_2$]	127.7–138.4 [m]
	8.7 [d, $^2J_{CP}$ = 7 Hz, $\underline{C}H_3CH_2$]	
	21.7 [m, Aryl–CH_3]	
	29.6 [m, CH_2]	
	37.5 [q, $^2J_{CP}$ = 6 Hz, C_q]	
	40.2 [m, $\underline{C}H_3C_q$]	
	222.5 [m, CO]	
5k	21.9 [s, Aryl–CH_3]	126.2–138.2 [m]
	30.7 [m, $\underline{C}H_2C_q$]	
	36.3 [q, $^2J_{CP}$ = 5.5 Hz, C_q]	
	39.5 [m, $\underline{C}H_3C_q$]	
	43.3 [m, $\underline{C}H_2Ph$]	
	222.5 [m, CO]	
5l	29.0 [m, CH_2P]	126.3–132.3 [m]
	40.2 [m, C_q]	
	43.9 [m, CH_2P]	
	222.1 [m, CO]	

[a] Solvent: $CDCl_3$; C_q ≡ quaternary C.

For the separation of the diastereomeric forms of **5d**, **k**, **l** the following procedure was carried out:

Table 17. MS (EI) data of compounds **5**

No.	(*m/z*) (%)	(*m/z*) (%)	(*m/z*) (%)	(*m/z*) (%)	(*m/z*) (%)
5e	930 (19)	904 (6)	876 (20)	757 (20)	729 (20)
	$[M^+]$	$[M^+ - CO]$	$[M^+ - 2CO]$	$[M^+ - 2CO, - CH_2(2,5\text{-}Me_2C_6H_3)]$	$[M^+ - 3CO, - CH_2(2,5\text{-}Me_2C_6H_3)]$
5f	998 (0.6)	970 (0.4)	942 (0.7)	914 (0.3)	773 (0.5)
	$[M^+]$	$[M^+ - CO]$	$[M^+ - 2CO]$	$[M^+ - 3CO]$	$[M^+ - 3CO, - CH_2(2\text{-naph.})]$
5g	890 (15)	862 (10)	834 (26)	806 (11)	715 (38)
	$[M^+]$	$[M^+ - CO]$	$[M^+ - 2CO]$	$[M^+ - 3CO]$	$[M^+ - 3CO, - CH_2Ph]$
5h	890 (8)	834 (23)	743 (22)	715 (18)	435 (76)
	$[M^+]$	$[M^+ - 2CO]$	$[M^+ - 2CO, - CH_2Ph]$	$[M^+ - 3CO, - CH_2Ph]$	$[M^+ - 3CO, - 3CH_2Ph, - Mo]$
5i	704 (35)	676 (26)	648 (100)	620 (95)	–
	$[M^+]$	$[M^+ - CO]$	$[M^+ - 2CO]$	$[M^+ - 3CO]$	
5j	746 (24)	718 (4)	690 (15)	662 (7)	–
	$[M^+]$	$[M^+ - CO]$	$[M^+ - 2CO]$	$[M^+ - 3CO]$	
5k	932 (33)	904 (13)	876 (34)	848 (10)	757 (56)
	$[M^+]$	$[M^+ - CO]$	$[M^+ - 2CO]$	$[M^+ - 3CO]$	$[M^+ - 3CO, - CH_2Ph]$
5l	924 (18)	896 (7)	868 (18)	792 (6)	749 (12)
	$[M^+]$	$[M^+ - CO]$	$[M^+ - 2CO]$	$[M^+ - 2CO, - Ph]$	$[M^+ - 3CO, - CH_2Ph]$

Table 18. IR, CV data and decomposition temperatures of compounds **5**

No.	IR (CH_2Cl_2) $\tilde{\nu}$ CO [a] (cm^{-1})	Decomposition temp. (°C)	CV $E_{1/2}$ (V)
5e	1931 (vs)	106	0.51
	1837 (vs)		
5f	1934 (vs)	300	0.51
	1844 (vs)		
5g	1933 (vs)	249	–
	1843 (vs)		
5h	1934 (vs)	243	0.49
	1844 (vs)		
5i	1934 (vs)	168	–
	1844 (vs)		
5j	1929 (vs)	90	–
	1844 (vs)		
5k	1932 (vs)	265	0.48
	1841 (vs)		
5l	1933 (vs)	196	–
	1837 (vs)		

[a] Local C_{3v} symmetry.

Table 19. Elemental analyses of compounds **5e**, **f**, **g**, **h**, **k**, **l**[a]

No.	chemical formula	elemental analysis	
5e	$C_{53}H_{57}MoO_3P_3$	C 67.06 (C 68.38)	H 6.34 (H 6.17)
5f	$C_{59}H_{51}MoO_3P_3$	C 68.92 (C 71.08)	H 5.58 (H 5.16)
5g	$C_{50}H_{51}MoO_3P_3$	C 64.52 (C 67.57)	H 5.65 (H 5.78)
5h	$C_{50}H_{51}MoO_3P_3$	C 67.31 (C 67.57)	H 6.04 (H 5.78)
5k	$C_{53}H_{57}MoO_3P_3$	C 66.90 (C 68.38	H 6.33 (H 6.17)
5l	$C_{53}H_{49}MoO_3P_3$	C 63.64 (C 69.98)	H 5.34 (H 5.35)

[a] Data in brackets are calculated.

A concentrated dichloromethane solution (10 ml) was divided between four test tubes (Ø = 1 cm), which were placed in a Schlenk tube (250 ml). Petroleum ether (40/60) was introduced into the tube. Vapor diffusion of the petroleum ether (40/60) yielded pale-yellow single crystals suitable for X-ray structure analysis.

2. From **6**: To a stirred solution of the ligand **6** (**6e**: 1.50 g, 2.00 mmol; **6f**: 1.63 g, 2.00 mmol; **6g**: 1.42 g, 2.00 mmol; **6h**: 1.42 g, 2.00 mmol; **6i**: 1.05 mg, 2.00 mmol; **6j**: 1.13 g, 2.00 mmol; **6k**: 1.50 g, 2.00 mmol; **6l**: 1.49 g, 2.00 mmol) in dichloromethane (50 ml), solid $(CH_3CN)_3Mo(CO)_3$[14] (670 mg, 2.20 mmol) was added. The solution immediately turned yellow. After stirring for 24 h, the brownish solution was filtered through Kieselgel (4 cm) and Kieselgur (2 cm). The stationary phase was treated with a dichloromethane/petroleum ether (40/60) mixture (ratio 5:1) until the eluent was colourless. Evaporation of the solvent and drying in vacuo for 2 d afforded compounds **5** as pale-yellow powders.

Yield: **5e**: 1.73 g (93%); **5f**: 1.85g (93%); **5g**: 1.63 g (92%); **5h**: 1.67 g (94%), **5i**: 1.22 mg (87%); **5j**: 1.36 g (91%); **5k**: 1.68 g (90%); **5l**: 1.62 g (88%).

For analytical data and preparation of compounds **5a**–**d** see ref.[12].

Table 20. ^{1}H- and ^{13}C-NMR data of compounds **6**[a]

No.	^{1}H NMR δ	^{13}C NMR δ
6e	0.92 [s, 3 H, CH_3C_q], 1.73–2.41 [m, 24 H, Aryl–CH_3, CH_2(2,5-$Me_2C_6H_3$)], 2.68–2.89 [m, 6 H, CH_2C_q], 6.90–7.33 [m, 24 H, aromatic H]	19.8, 21.3 [s, Aryl–CH_3], 28.6 [m, CH_3C_q], 34.8 [s, C_q], 36.5 [m, CH_2(2,5-$Me_2C_6H_3$)], 126.9–133.8 [m, aromatic C]
6f	0.88 [s, 3 H, CH_3C_q], 1.78–2.15 [m, 6 H, CH_2(2-naph.)], 2.83–3.11 [m, 6 H, CH_2C_q], 6.99–7.78 [m, 36 H, aromatic H]	29.8 [m, CH_3], 38.2 [m, CH_2(2-naph.), C_q], 42.3 [m, CH_2C_q], 125.5–139.8 [m, aromatic C]
6g	0.81 [m, 3 H, CH_3C_q], 1.77–2.22 [m, 6 H, CH_2Ph], 2.32–2.36 [m, 9 H, Aryl–CH_3], 2.66–3.05 [m, 6 H, CH_2C_q], 6.79–7.55 [m, 27 H, aromatic H]	21.8 [s, Aryl–CH_3], 26.1 [s, CH_3C_q], 38.4 [m, CH_2Ph, C_q], 42.0 [m, CH_2C_q], 125.9–139.2 [m, aromatic C]
6h	1.00 [m, 3 H, CH_3C_q], 1.80–3.00 [m, 21 H, CH_2, Aryl–CH_3], 6.98–7.45 [m, 27 H, aromatic H]	21.2 [s, Aryl–CH_3], 29.2 [q, $^3J_{CP}$ = 9.5 Hz, CH_3C_q], 38.6 [m, CH_2Ph, C_q], 42.5 [m, CH_2C_q], 125.9–144.3 [m, aromatic C]
6i	1.00 [m, 3 H, CH_3C_q], 1.14–1.31 [m, 9 H, CH_3P], 2.25–2.72 [m, 6 H, CH_2P], 2.25–2.31 [m, 18 H, Aryl–CH_3], 6.71–7.65 [m, 9 H, aromatic H]	21.7 [s, Aryl–CH_3], 25.8 [s, CH_3P], 29.6 [m, CH_3C_q], 37.8 [m, C_q], 40.1 [m, CH_2C_q], 128.5–140.9 [m, aromatic C]
6j	0.73–1.16 [m, 9 H, CH_2CH_3], 0.95 [s, 3 H, CH_3C_q], 1.45–2.70 [m, 12 H, CH_2], 2.27–2.32 [m, 18 H, Aryl–CH_3], 6.95–7.27 [m, 9 H, aromatic H]	10.8 [d, $^2J_{CP}$ = 3.6 Hz, CH_2CH_3], 21.7 [s, Aryl–CH_3], 23.0 [m, CH_2CH_3], 29.4 [m, CH_3C_q], 38.4 [m, C_q], 42.9 [m, CH_2C_q], 129.3–140.0 [m, aromatic C]
6k	0.87 [m, 3 H, CH_3C_q], 1.72–2.14 [m, 6 H, CH_2Ph], 2.26–2.34 [m, 18 H, Aryl–CH_3], 2.65–3.17 [m, 6 H, CH_2C_q], 6.85–7.27 [m, 24 H, aromatic H]	21.7 [s, Aryl–CH_3], 28.9 [m, CH_3C_q], 38.3 [m, CH_2Ph, C_q], 41.8 [m, CH_2C_q], 125.9–138.8 [m, aromatic C]
6l	1.57–2.05 [m, 6 H, PCH_2Ph], 2.49–3.10 [m, 6 H, C_qCH_2P], 2.95 [s, 2 H, $PhCH_2C_q$], 6.6–7.3 [m, 20 H, aromatic H]	38.0 [m, CH_2], 42.7 [m, CH_2], 45.8 [m, C_q], 126.1–134.8 [m, aromatic C]

[a] Solvent: $CDCl_3$; C_q ≡ quaternary C.

For further analytical data see Tables 8–11.

Compounds **6**, $RCH_2C[CH_2P(Ar)(R')]_3$: To a stirred solution of the ligand **2** (**2a**: 1.00 g, 2.5 mmol; **2b**,**c**: 1.10 g, 2.5 mmol; **2d**: 1.20 g, 2.5 mmol; **2e**: 1.18 g, 2.5 mmol) in THF (60 ml), methyllithium (1.6 M in diethyl ether, 4.70 ml; 7.50 mmol) was slowly added at 0°C. The colourless solution turned red. The solution was al-

Table 21. ^{31}P-NMR data of compounds **6**[a]

No.	^{31}P NMR δ
6e	(–33.4) – (–33.5) (m)
6f	(–29.9) – (–30.1) (m)
6g	(–29.5) – (–29.8) (m)
6h	(–44.1) – (–44.4) (m)
6i	(–47.5) – (–49.2) (m)
6j	(–31.6) – (–32.0) (m)
6k	(–28.8) – (–29.1) (m)
6l	(–29.2) – (–29.4) (m)

[a] Solvent: $CDCl_3$.

Table 22. MS (EI) data of compounds **6**

No.	(*m/z*) (%)	(*m/z*) (%)	(*m/z*) (%)	(*m/z*) (%)	(*m/z*) (%)
6e	751 (14)	631 (100)	–	–	–
	$[M^+]$	$[M^+ - CH_2(2,5\text{-}Me_2C_6H_3), -CH_3]$			
6f	817 (11)	691 (23)	675 (85)	549 (100)	423 (82)
	$[M^+]$	$[M^+ - (2\text{-naph.})]$	$[M^+ - CH_2(2\text{-naph.})]$	$[M^+ - (2\text{-naph.}), -CH_2(2\text{-naph.})]$	$[M^+ - 2(2\text{-naph.}), -CH_2(2\text{-naph.})]$
6g	708 (20)	616 (100)	435 (35)	–	–
	$[M^+]$	$[M^+ - CH_2Ph, -H]$	$[M^+ - 3CH_2Ph]$		
6h	707 (4)	617 (100)	435 (43)	–	–
	$[M^+ - H]$	$[M^+ - CH_2Ph]$	$[M^+ - 3CH_2Ph]$		
6i	521 (2)	507 (100)	–	–	–
	$[M^+ - H]$	$[M^+ - CH_3]$			
6j	564 (1)	536 (100)	–	–	–
	$[M^+]$	$[M^+ - C_2H_5, +H]$			
6k	659 (100)	583 (31)	477 (40)	–	–
	$[M^+ - CH_2Ph]$	$[M^+ - CH_2Ph, -Ph, -H]$	$[M^+ - CH_2Ph, -Ph, -(3,5\text{-}Me_2C_6H_3, +3H]$		
6l	742 (15)	651 (100)	575 (52)	–	–
	$[M^+]$	$[M^+ - CH_2Ph]$	$[M^+ - CH_2Ph, -Ph, +H]$		

lowed to warm to room temperature and stirred for 2 h. Subsequently, the solution was cooled to 0°C once more and the alkyl halide [**6e**: $ClCH_2(2,5\text{-}Me_2C_6H_3)$, 1.16 g, 7.5 mmol; **6f**: $BrCH_2$(2-naph.), 1.66 g, 7.5 mmol; **6g**, **h**, **k**, **l**: $ClCH_2Ph$, 950 mg, 7.5 mmol; **6i**: MeI, 1.10 g, 7.5 mmol; **6j**: EtBr, 820 mg, 7.5 mmol] was slowly added. Following the addition of the alkyl halide, the mixture was warmed to room temperature and stirred for a further 2 h. The solvent was then removed and the remaining residue was suspended in toluene (20 ml). Filtration through Kieselgur (2 cm) afforded a clear solution. On evaporation of the solvent, the ligands **6** were obtained as oils (**6e**, **g**, **i**, **j**, **k**) or powders (**6f**, **h**, **l**).

Yield: **6e**: 1.81 g (96%); **6f**: 1.72 g (84%); **6g**: 1.56 g (96%); **6h**: 1.42 g (87%); **6i**: 1.00 g (91%); **6j**: 1.10 g (93%); **6k**: 1.21 g (77%); **6l**: 1.23 g (92%).

X-ray Crystal Structure Determination: The measurements were made on a Siemens P4 four-circle diffractometer using graphite-monochromated Mo-K_α radiation. The intensities of three check reflections (measured every 100 reflections) remained constant throughout the data collection, thus indicating crystal and electronic stability. All calculations were performed using the SHELXTL-PLUS[16] software package. Structures were solved by direct methods with the SHELXL-93[17] program. The graphical handling of the structural information during solution and refinement was performed using XPMA[18]. Absorption corrections (Ψ scan, $\Delta\Psi = 10°$) were applied to the data. The structures were refined in fully or partially anisotropic models by full-matrix least-squares procedures with hydrogen atoms introduced at calculated positions. Data relevant to the structure determinations are compiled in Table 23. Peculiarities about the structures are as follows: **5l**: there is some disorder in the orientation of the phenyl group of the benzyl residue bound to the quaternary carbon. The major rotamer is shown in Figure 10. This disorder is not completely resolved; it accounts for the high residual electron density observed in this region, as well as for the relatively high R-factors.

Further details of the crystal structure investigations may be obtained from the Fachinformationszentrum Karlsruhe, D-76344 Eggenstein-Leopoldshafen (Germany), on quoting the depository numbers CSD-407026 (**5d**), CSD-407025 (**5k**), and CSD-407027 (**5l**).

Table 23. Summary of data related to crystallography, data collection and refinement of **5d**, **k**, **l**

Compound	**5d**	**5k**	**5l**
Chemical formula	$C_{47}H_{45}MoO_3P_3$	$C_{53}H_{57}MoO_3P_3$	$C_{53}H_{46}MoO_3P_3$
Formula mass	846.7	930.8	919.8
Crystal system	monoclinic	monoclinic	monoclinic
Space group	$P2_1/c$	C_2	$P2_1/n$
a [Å]	21.503 (6)	24.845 (6)	9.331 (1)
b [Å]	9.233 (3)	8.893 (1)	25.725 (5)
c [Å]	21.442 (6)	23.424 (3)	20.793 (4)
α [°]	90.00 (0)	90.00(0)	90.00 (0)
β [°]	76.72 (1)	81.49 (1)	102.15 (1)
γ [°]	90.00 (0)	90.00 (0)	90.00 (0)
V [Å^3]	4143 (2)	5119 (2)	4879 (2)
Z	4	4	4
ρ(calcd.) [g/cm^3]	1.357	1.272	1.252
μ [mm^{-1}]	0.47	0.45	0.41
F(000)	1752	2040	1900
Temperature [K]	200	200	200
Crystal size [mm]	0.1 × 0.2 × 0.2	0.2 × 0.3 × 0.3	0.2 × 0.3 × 0.3
Index range	$0 \le h \le 23$ $0 \le k \le 10$ $-22 \le l \le 23$	$0 \le h \le 29$ $0 \le k \le 11$ $-29 \le l \le 29$	$0 \le h \le 11$ $0 \le k \le 30$ $24 \le l \le 24$
Theta range	$3.9° \le 2\theta \le 46.0°$	$3.3° \le 2\theta \le 54.0°$	$2.6° \le 2\theta \le 50.0°$
Data-collecting mode	ω-scan; Δω = 0.60°	ω-scan; Δω = 0.60°	ω-scan; Δω = 0.60°
Speed (°min^{-1})	$10.0 \le \dot{\theta} \le 60.0$	$10.0 \le \dot{\theta} \le 30.0$	$10.0 \le \dot{\theta} \le 10.0$
Refl. collected	5932	5937	9147
Refl. unique	5755	5745	8579
Refl. observed ($I > 2\sigma$)	3093	4255	4502
No. variables	483	580	561
Larg. res. peak [e/Å^3]	0.55	1.03	5.6
Final R ($I > 2\sigma$)	7.2%	6.8%	13.2%
Final $wR2$	22.3%	20.4%	44.1%

[1] S. Beyreuther, J. Hunger, G. Huttner, S. Mann, L. Zsolnai, *Chem. Ber.* **1996**, *129*, 745.

[2] [2a] M. Di Vaira, L. Sacconi, *Angew. Chem.* **1982**, *94*, 338; *Angew. Chem. Int. Ed. Engl.* **1982**, *21*, 330. – [2b] M. di Vaira, S. Midollini, L. Sacconi, *J. Am. Chem. Soc.* **1979**, *101*, 1757. – [2c] M. Di Vaira, M. Peruzzini, P. Stoppioni, *J. Chem. Soc., Dalton Trans.* **1984**, 359. – [2d] M. Di Vaira, P. Innocenti, S. Moneti, M. Peruzzini, P. Stoppioni, *Inorg. Chim. Acta* **1984**, *83*, 161.

[3] [3a] C. Bianchini, A. Meli, M. Peruzzini, F. Vizza, P. Frediani, J. A. Ramirez, *Organometallics* **1990**, *9*, 226. – [3b] C. Bianchini, A. Meli, M. Peruzzini, F. Vizza, A. Albinati, *Organometallics* **1990**, *9*, 2283. – [3c] J. Ott, G. M. Ramos Tombo, B. Schmid, L. M. Venanzi, G. Wang, T. R. Ward, *Tetrahedron Lett.* **1989**, *30*, 6151. – [3d] J. Ott, B. Schmid, L. Venanzi, G. Wang, T. R. Ward, G. M. Ramos Tombo, *New J. Chem.* **1990**, *40*, 495. – [3e] V. Sernau, G. Huttner, M. Fritz, L. Zsolnai, O. Walter, *J. Organomet. Chem.* **1993**, *453*, C23. – [3f] E. G. Thaler, K. Folting, K. G. Caulton, *J. Am. Chem. Soc.* **1990**, *112*, 2664. – [3g] M. J. Burk, J. E. Feaster, R. L. Harlow, *Tetrahedron: Asymmetry* **1991**, *2*, 569.

[4] [4a] S.-T. Liu, H.-E. Wang, M.-C. Cheng, S.-M. Peng, *J. Organomet. Chem.* **1989**, *376*, 333. – [4b] S.-T. Liu, K.-J. Liu, *Inorg. Chem.* **1990**, *29*, 4576. – [4c] S.-T. Liu, C.-L. Tsao, M.-C. Cheng,

S.-M. Peng, *Polyhedron* **1990**, *9*, 2579. – [4d] S.-T. Liu, *J. Chin. Chem. Soc.* **1992**, *39*, 611. – [4e] G. Reinhard, R. Soltek, G. Huttner, A. Barth, O. Walter, L. Zsolnai, *Chem. Ber.* **1996**, *129*, 97. – [4f] T. Seitz, A. Muth, G. Huttner, *Chem. Ber.* **1994**, *127*, 1837. – [4g] T. Seitz, A. Muth, G. Huttner, *Z. Naturforsch., B: Chem. Sci.* **1995**, *50*, 1045.

[5] [5a] H. Heidel, G. Huttner, G. Helmchen, *Z. Naturforsch., B: Chem. Sci.* **1993**, *48*, 1681. – [5b] H. Heidel, G. Huttner, R. Vogel, G. Helmchen, *Chem. Ber.* **1994**, *127*, 271. – [5c] H. Heidel, G. Huttner, L. Zsolnai, *Z. Naturforsch., B: Chem. Sci.* **1995**, *50*, 729.

[6] M. J. Burk, R. L. Harlow, *Angew. Chem.* **1990**, *84*, 1070; *Angew. Chem. Int. Ed. Engl.* **1990**, *29*, 1647.

[7] T. R. Ward, L. M. Venanzi, A. Albinati, F. Lianza, T. Gerfin, V. Gramlich, G. M. Ramos Tombo, *Helv. Chim. Acta* **1991**, *74*, 983.

[8] [8a] K. Issleib, H. O. Fröhlich, *Z. Naturforsch.* **1959**, *14b*, 349. – [8b] K. Issleib, A. Tzschach, *Chem. Ber.* **1959**, 1118.

[9] B. R. Kimpton, W. McFarlane, A. S. Muir, P. G. Patel, *Polyhedron* **1993**, *12*, 2525.

[10] Th. Klein, *Dissertation*, Universität Heidelberg, **1990**.

[11] O. Walter, Th. Klein, G. Huttner, L. Zsolnai, *J. Organomet. Chem.* **1993**, *458*, 63.

[12] [12a] W. Hewertson, H. R. Watson, *J. Chem. Soc.* **1962**, 1490. – [12b] A. Muth, O. Walter, G. Huttner, A. Asam, L. Zsolnai, Ch. Emmerich, *J. Organomet. Chem.* **1994**, *468*, 149. – [12c] A. Asam, Doctorate Thesis, Universität Heidelberg, **1994**. – [12d] P. Schober, Doctorate Thesis, Universität Heidelberg, in preparation.

[13] D. P. Tate, W. R. Knipple, J. M. Augl, *Inorg. Chem.* **1962**, *1*, 433.

[14] WIN-DAISY 3.0, Version 950815, Bruker, **1996**.

[15] MOLECULAR SIMULATIONS (MS), Insight II, Version 4.0.0, San Diego **1996**.

[16] SHELXLTL-PLUS, G. M. Sheldrick, Universität Göttingen, **1988**.

[17] SHELXL-93, G. M. Sheldrick, Universität Göttingen, **1993**.

[18] XPMA, L. Zsolnai, Universität Heidelberg, **1997**.

[97138]